

# Coherent control of exciton-polariton vortices in a patterned GaAs microcavity

Gaël Nardin, Konstantinos G. Lagoudakis, Barbara Pietka,  
François Morier-Genoud, Yoan Léger, Benoît Deveaud-Plédran  
*Laboratoire d'Optoélectronique Quantique, École Polytechnique Fédérale  
de Lausanne (EPFL), Station 3, CH-1015 Lausanne, Switzerland.*

Exploiting the geometrical properties of exciton-polaritons confined in circular traps, we experimentally demonstrate the creation of quantized vortices in the coherent polariton field. These vortical states, carrying an integer angular orbital momentum  $m$ , are natural eigenstates of the trapped polariton gas. Coherent control allows us to select the charge of the vortex. In this way, the injection of singly charged ( $m = 1$  &  $m = -1$ ) and doubly charged ( $m = 2$ ) vortices is shown. This work demonstrates the possibility of creating quantized vortices in a polariton gas although the system is driven in the linear regime.

The generation of optical vortices has been demonstrated in different types of lasers ranging from ring resonators [1] to Vertical Cavity Surface Emitting Lasers (VCSELs) [2, 3]. These vortical entities have been topologically compared with the vortices encountered in superfluid systems [1, 4]. In our contribution, we use a semiconductor microcavity where the optical modes are strongly coupled to the excitonic resonance of a quantum well (QW). In this case, due to a normal mode splitting, the eigenmodes of the system are not the bare cavity or exciton modes any more, but are new eigenmodes called upper and lower polaritons (UP and LP), separated in energy by the characteristic vacuum Rabi splitting [5]. Using the geometry of confined polariton modes, we demonstrate the creation of exciton-polariton quantized vortices. So far, polariton quantized vortices have been observed in the Bose-condensed phase of 2D microcavity polaritons [6], where they are pinned by the natural disorder present in the cavity. The two characteristics of quantized vortices have been observed: a rotation of the phase around the vortex core by an integer multiple of  $2\pi$ , and a minimum of the fluid density at the core. The presence of these vortices has been interpreted as a sign of superfluidity [7]. We show here that exciton-polariton vortices can be produced by geometrical means in the linear regime, and can be controlled using selective resonant excitation of the polariton modes.

The sample under study is a patterned GaAs  $\lambda$ -cavity with one embedded InGaAs QW, sandwiched between two semiconductor distributed bragg reflectors (DBRs), featuring a vacuum Rabi splitting of  $3.5$  meV. Our traps consist of quasi-circular mesas that were etched on the microcavity spacer, in order to create a lateral confining potential for the cavity electromagnetic field [8]. This potential produces confinement for both the upper and lower polariton branches, leading to discrete confined polariton states. The linewidth of these states is of the order of  $80\mu\text{eV}$ . All measurements presented in the paper were performed on lower polariton states confined in mesas of  $9\mu\text{m}$  diameter, and for a detuning of  $\delta \sim 0$  meV between the confined photonic mode and the excitonic resonance

( $1.484\text{eV}$ ). Similar results were obtained in traps with diameters varying between  $3\mu\text{m}$  and  $20\mu\text{m}$ , as well as on the confined UP branch.

A spatially resolved spectrum of the photoluminescence emitted by the confined states under non-resonant pumping is shown in Figure 1 (a). Discrete eigenstates can be observed for the lower polariton branch (below  $1.484\text{eV}$ ) and the upper polariton branch (above  $1.484\text{eV}$ ). The confined eigenstates can be labeled after a particle-in-a-box picture by two quantum numbers  $(n, m)$ , with  $n = 1, 2, 3, \dots$  and  $m = 0, \pm 1, \pm 2, \dots$  [9, 10]. In polar coordinates,  $n$  gives the number of lobes of the wavefunction in the radial direction. For a given quantum number  $m$ , the state undergo a phase rotation of  $e^{im\phi}$  in the azimuthal direction. The  $\pm m$  states are degenerate due to the cylindrical symmetry of the system.

Imaging wavefunctions of confined polaritons is possible by means of optical microscopy. Indeed, due to their very small effective mass ( $10^4$  times smaller than the free electron mass), polaritons can be confined in traps of sizes in the micrometer range, above the optical resolution limit. Images of the two-dimensional distribution of the confined state probability densities can be realized either using a tomography technique [9], or by directly imaging the coherent emission of a given state when it is resonantly excited with a continuous wave laser [10]. The emission intensity gives direct information on the probability density of the polariton states.

To image the wavefunction rather than the probability density only, one needs a phase-resolved detection scheme. In this perspective, we used a homodyne detection setup, where we split the  $cw$  pump laser into two. One part was focalized on the back side of the sample in a gaussian spot of  $\sim 15\mu\text{m}$  diameter to resonantly excite the polariton states, the other part served as a phase reference. The coherent emission of the polariton state was then collected from the front side using a  $0.5$  N.A. microscope objective, interfered with the reference beam, and imaged on a CCD. Figure 1 (b) shows the emission of the ground state ( $n = 1, m = 0$ ) of the lower confined polariton [indicated with a plain arrow in Fig. 1 (a)] interfer-

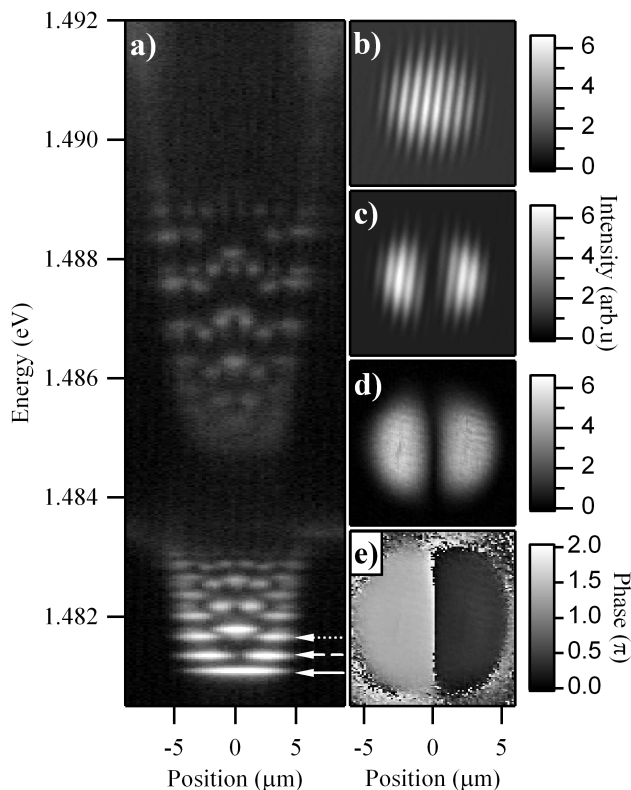


FIG. 1. (a) Photoluminescence intensity emitted by the confined polariton states in a trap of  $9\mu\text{m}$  in diameter, under non-resonant pumping (at  $1.57\text{ eV}$ , in the first minimum of reflection of the DBR), in a logarithmic scale. Confined lower (upper) polariton states are visible below (above)  $1.484\text{ eV}$ . (b) Interferogram resulting from the interference of the coherent emission of the lower polariton ground state ( $n = 1, m = 0$ ) with the reference laser. (c),(d) and (e) are respectively the interferogram, the wavefunction amplitude and wavefunction phase of the lower polariton first excited state ( $n = 1, m = \pm 1$ ).

ing with the reference laser. A slightly different incidence angle is used for the signal and the reference, to provide straight interference fringes. As the ( $n = 1, m = 0$ ) state is expected to have a constant phase, the phase gradient obtained with this state is used as a phase reference for the other interferograms. Using numerical Fourier transform and off-axis filtering[11], one can then extract the amplitude and phase of the polariton states. The high contrast of the resulting interference fringes over the whole emission pattern is the signature of a coherent polariton field.

The interferogram of the first excited state ( $n = 1, m = \pm 1$ ) [indicated with a dashed arrow in Fig. 1 (a)] is shown in Fig. 1 (c). We have extracted the amplitude [Fig. 1 (d)] and the phase [Fig. 1 (e)] of the polariton wavefunction. In Fig. 1 (e), the  $\pi$ -phase shift between the two lobes is clearly visible. It indicates that the left lobe of the wavefunction is of opposite sign than the right lobe.

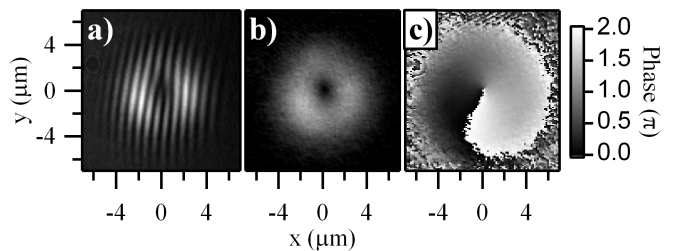


FIG. 2. (a) Interferogram resulting from the interference of the coherent emission of the ( $n = 1, m = +1$ ) state of the lower polariton with the reference laser, displaying a clear fork-like dislocation. (b) Amplitude of the coherent polariton field, extracted from (a), showing a minimum in the field density at the place of the phase singularity. (d) Phase of the coherent polariton field, extracted from (a), indicating a  $2\pi$ -phase shift rotation of the phase around the singularity.

Around the trap the phase is not defined, as the wavefunction is exponentially decaying outside the trap.

The two-lobe pattern of the first excited state in Fig. 1 (c)-(e) indicates a fixed phase relationship between the  $m = \pm 1$  states [10]. In the most general case, the azimuthal dependence of the wavefunction in circular boundary conditions reads as:

$$\psi(\phi) = A\psi_{+m}(\phi) + B\psi_{-m}(\phi) = Ae^{im\phi} + Be^{-im\phi}$$

where  $A$  and  $B$  are complex coefficients. For example, one obtains the pattern shown in Fig. 1 (d) and (e) when  $A = B = \frac{1}{\sqrt{2}}$  and  $m = 1$ . The value of coefficients  $A$  and  $B$  is given by the overlap (in real space, reciprocal space and energy) between the  $\pm m$  states and the pump: the excitation laser can be used to lock, and subsequently control, the interference pattern in any arbitrary direction [10]. We are going to show that by carefully selecting certain pumping conditions one can create “pure”  $+m$  or  $-m$  states, carrying an integer angular orbital momentum.

Such a state is experimentally produced and shown in Fig. 2 for ( $n = 1, m = +1$ )[12]. In the interferogram displayed in Fig. 2 (a), one can observe a very clear fork-like dislocation, indicating the presence of a phase singularity. We extract from this interferogram the amplitude [Fig. 2 (b)] and phase [Figure 2 (c)] of the polariton field. The intensity minimum at the center of the trap (b) and the  $2\pi$ -phase shift around the core (c) are straightforwardly visible. The core of this vortex is situated at the center of the trap, and the size of the vortex is delimited by the mesa diameter.

In the following, we show that such a  $m = +1$  vortex state can be created by focusing the excitation laser on the side of the trap, with a finite excitation angle. These experimental conditions allow to inject polaritons with a well defined in-plane momentum mainly on one side of the trap. This can be used to select which of the  $+m$  or  $-m$  state is injected. Indeed, depending on the side of the

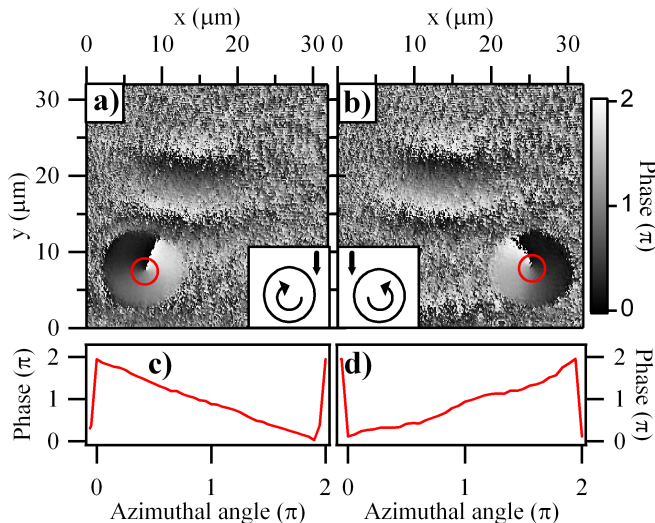


FIG. 3. (color online) Phase mapping (a) and phase distribution along the red circle (c) of the polariton gas in the trap, when the polaritons are injected on the right side of the mesa using a pump angle of around  $4^\circ$ . In this configuration, the vortex is rotating clockwise. (b-d) Same as (a-c), but injection on the left side of the mesa. In this configuration, the vortex is rotating counterclockwise. Insets: schematic view of the vortex rotation, the pump and its in-plane direction are represented by the thick arrow.

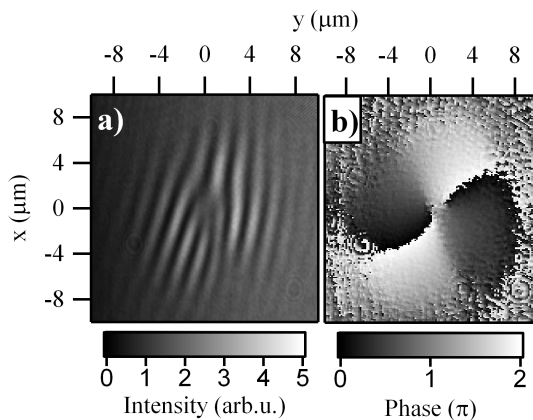


FIG. 4. (a) Interferogram resulting from the interference of the coherent emission of the lower polariton second excited state ( $n = 1, m = +2$ ) with the reference laser, displaying a trident-like dislocation. (b) Phase mapping extracted from (a), displaying a double vortex structure.

trap on which the laser is focused, the charge is going to be positive or negative, as demonstrated in Fig. 3. The phase distribution [Fig. 3, (a)-(b)] and the phase profile along the red circle [Fig. 3, (c)-(d)] are displayed when the mesa is positioned on the left side [Fig. 3 (a)-(c)] or right side [Fig. 3 (b)-(d)] of the excitation spot. It is interesting to note that this selective excitation scheme is compatible with the picture of the injection of a polariton

fluid in the trap. The treatment of the polariton field as a propagating fluid has been recently highlighted in Ref. [13].

It is also possible to control the value of the vortex charge, by exciting a state with another quantum number  $m$ . Figure 4 displays the interferogram [Fig. 4 (a)] and corresponding phase mapping [Fig. 4 (b)] of a ( $n = 1, m = +2$ ) state [indicated with a dotted arrow in Fig. 1 (a)]. A trident-like dislocation is visible in the interferogram, resulting in a  $4\pi$ -phase shift around the core.

In conclusion, we have demonstrated the creation and control of trapped vortices in a patterned semiconductor microcavity. By operating in the linear regime, we show that quantized vortices in a polariton field can be also observed in a non-degenerate gas, in absence of superfluidity. Thanks to the homodyne detection setup, the phase and the amplitude of the coherent polariton gas were directly visualized. We have experimentally shown the control of the vortex charge. This work shows the essential role of engineered lateral confinement to tailor the wavefunction and the subsequent emission pattern of a coherently controlled exciton-polariton gas. Going beyond the linear regime [14] to exploit the matter part of these confined polariton vortices is the next natural step, which will possibly provide new exploitation schemes for polariton lasers [15].

We would like to thank T.K Paraíso, R. Cerna, M.T. Portella-Oberli, O. El Daif, N. Pavillon and B. Caire-Remonnay for helpful discussions. We acknowledge support by the Swiss National Research Foundation through the NCCR Quantum Photonics.

- 
- [1] M. Brambilla, F. Battipede, L.A. Lugiato, V. Penna, F. Prati, C. Tamm, and C.O. Weiss, *Phys. Rev. A* **43**, 5090 (1990).
  - [2] F.B. de Colstoun, G. Khitrova, A.V. Fedorov, T.R. Nelson, C. Lowry, T.M. Brennan, B. Gene Hammons, and P.D. Maker, *Chaos Soliton Fractal* **4**, 1575 (1994).
  - [3] J. Scheuer and M. Orenstein, *Science* **285**, 230 (1999).
  - [4] P. Couillet, L. Gil, and F. Rocca, *Opt. Commun.* **73**, 403 (1989).
  - [5] C. Weisbuch, M. Nishioka, A. Ishikawa, and Y. Arakawa, *Phys. Rev. Lett.* **69**, 3314 (1992).
  - [6] K.G. Lagoudakis, M. Wouters, M. Richard, A. Baas, I. Carusotto, R. André, Le Si Dang, and B. Deveaud-Plédran, *Nature Phys.* **4**, 706 (2008).
  - [7] J. Keeling and N.G. Berloff, *Nature* **457**, 273 (2009).
  - [8] O. El Daif, A. Baas, T. Guillet, J.-P. Brantut, R. Idrissi Kaitouni, J. L. Staehli, F. Morier-Genoud, and B. Deveaud, *Appl. Phys. Lett.* **88**, 061105 (2006).
  - [9] G. Nardin, T. K. Paraíso, R. Cerna, B. Pietka, Y. Léger, O. El Daif, F. Morier-Genoud, and B. Deveaud, *Appl. Phys. Lett.* **94**, 181103 (2009).
  - [10] R. Cerna, D. Sarchi, T. K. Paraíso, G. Nardin, Y. Léger, M. Richard, B. Pietka, O. El Daif, F. Morier-Genoud, V.

Savona, M. T. Portella-Oberli, and B. Deveaud-Plédran, Phys. Rev. B **80**, 121309 (2009).

- [11] This technique is known as Off-Axis Digital Holography. See for example: E. Cuhe, P. Marquet, and C. Depeursinge, Appl. Optics **38**, 6994 (1999).
- [12] In some of the mesas, due to a slight ellipticity of the trap, there is a small degeneracy lifting of the  $\pm m$  doublet into two new eigenstates  $\frac{1}{\sqrt{2}}[\psi_{+m} \pm \psi_{-m}]$  [8–10]. This splitting being smaller than the linewidth, one can still excite a combination of the two split states, in order to create pure  $+m$  or  $-m$  states.
- [13] A. Amo, D. Sanvitto, F.P. Laussy, D. Ballarini, E. del Valle, M. D. Martin, A. Lemaître, J. Bloch, D. N. Krizhanovskii, M.S. Skolnick, C. Tejedor, and L. Viña, Nature **457**, 291 (2009).
- [14] G. Nardin, O. El Daif, T. K. Paraíso, A. Baas, M. Richard, F. Morier-Genoud, and B. Deveaud, Phys. Stat. Sol. (c) **5**, 2437 (2008).
- [15] D. Bajoni, P. Senellart, E. Wertz, I. Sagnes, A. Miard, A. Lemaître, and J. Bloch, Phys. Rev. Lett. **100**, 047401 (2008).